OFFICE OF NAVAL RESEARCH

Contract N00014-82K-0612

Task No. NR 627-838

TECHNICAL REPORT NO. 61

Effect of Reagent Concentrations Used to Synthesize Polypyrrole on the Chemical Characteristics and Optical and Electronic Properties of the Resulting Polymer

by

Junting Lei, Zhihau Cai and Charles R. Martin

Department of Chemistry
Colorado State University
Ft. Collins, CO 80523

Prepared for publication

in

Synthetic Metals

July 18, 1991

REPORT DOCUMENTATION PAGE

OMB No. 0704-0188

1a. REPORT SECURITY CLASSIFICATION UNCLASSIFIED	1b. RESTRICTIVE MARKINGS
2a. SECURITY CLASSIFICATION AUTHORITY	3. DISTRIBUTION/AVAILABILITY OF REPORT APPROVED FOR PUBLIC DISTRIBUTION, DISTRIBUTION UNLIMITED.
2b. DECLASSIFICATION/DOWNGRADING SCHEDULE	
4. PERFORMING ORGANIZATION REPORT NUMBER(S) ONR TECHNICAL REPORT #61	5. MONITORING ORGANIZATION REPORT NUMBER(S)
6a. NAME OF PERFORMING ORGANIZATION Dr. Charles R. Martin Department of Chemistry 6b. OFFICE SYMBOL (If applicable)	7a. NAME OF MONITORING ORGANIZATION Office of Naval Research
6c. ADDRESS (City, State, and ZIP Code) Colorado State University Ft. Collins, CO 80523	7b. ADDRESS (City, State, and ZIP Code) 800 North Quincy Street Arlington, VA 22217
8a. NAME OF FUNDING/SPONSORING ORGANIZATION Office of Naval Research 8b. OFFICE SYMBOL (If applicable)	9. PROCUREMENT INSTRUMENT IDENTIFICATION NUMBER Contract # N00014-82K-0612
8c. ADDRESS (City, State, and ZIP Code) 800 North Quincy Street Arlington, VA 22217	10. SOURCE OF FUNDING NUMBERS PROGRAM ELEMENT NO. / PROJECT NO. / TASK NO / WORK UNIT ACCESSION NO

11. TITLE (Include Security Classification)

Effect of Reagent Concentrations Used to Synthesize Polypyrrole on the Chemical Characteristic and Optical and Electronic Properties of the Resulting Polymer

12. PERSONAL AUTHOR(S)

Junting Lei, Zhihau Cai and Charles R. Martin

13a. TYPE OF REPORT	13b. TIME COVERED	14. DATE OF REPORT (Year, Month, Day)	15. PAGE COUNT
Technical	FROM _____ TO _____	(91,7,18) July 18, 1991	

16. SUPPLEMENTARY NOTATION

17 COSATI CODES		
FIELD	GROUP	SUB-GROUP

18. SUBJECT TERMS (Continue on reverse if necessary and identify by block number)

Electronically conductive polymers, polypyrrole, synthetic metals

19. ABSTRACT (Continue on reverse if necessary and identify by block number)

The objectives of the work described in this paper were to correlate conditions used to synthesize polypyrrole with the chemical characteristics of the resulting polymer, and then to correlate these chemical characteristics with electronic and optical properties of the polymer. The polypyrrole samples were synthesized from aqueous solutions of Fe^{3+} and pyrrole. Samples with differing chemical characteristics were obtained by varying the initial concentrations of Fe^{3+} and pyrrole in the polymerization solutions. The initial concentrations of Fe^{3+} in all polymerization solutions was 50 times higher than the initial concentration of pyrrole in the solution. However, the initial concentrations of Fe^{3+} and pyrrole varied from 2.0 M Fe^{3+}/0.04 M pyrrole to 0.06 M Fe^{3+}/0.0013 M pyrrole. This yielded polypyrrole samples having different chain and conjugation lengths and different concentrations of chemical defect sites. We show that both electronic and optical conductivity are affected by these changes in conjugation length and concentrations of chemical defects.

20. DISTRIBUTION/AVAILABILITY OF ABSTRACT ☒ UNCLASSIFIED/UNLIMITED ☐ SAME AS RPT. ☒ DTIC USERS	21. ABSTRACT SECURITY CLASSIFICATION UNCLASSIFIED
22a. NAME OF RESPONSIBLE INDIVIDUAL Dr. Robert Nowak	22b TELEPHONE (Include Area Code) (202) 696-4410 22c. OFFICE SYMBOL

DD Form 1473, JUN 86 Previous editions are obsolete. SECURITY CLASSIFICATION OF THIS PAGE

EFFECT OF REAGENT CONCENTRATIONS USED TO SYNTHESIZE POLYPYRROLE ON THE CHEMICAL CHARACTERISTICS AND OPTICAL AND ELECTRONIC PROPERTIES OF THE RESULTING POLYMER

Junting Lei, Zhihua Cai, and Charles R. Martin*

Department of Chemistry
Colorado State University
Fort Collins, CO 80523

A-1

*Corresponding author

ABSTRACT

The objectives of the work described in this paper were to correlate conditions used to synthesize polypyrrole with the chemical characteristics of the resulting polymer, and then to correlate these chemical characteristics with electronic and optical properties of the polymer. The polypyrrole samples were synthesized from aqueous solutions of Fe^{3+} and pyrrole. Samples with differing chemical characteristics were obtained by varying the initial concentrations of Fe^{3+} and pyrrole in the polymerization solutions. The initial concentration of Fe^{3+} in all polymerization solutions was 50 times higher than the initial concentration of pyrrole in the solution. However, the initial concentrations of Fe^{3+} and pyrrole varied from 2.0 M Fe^{3+}/0.04 M pyrrole to 0.06 M Fe^{3+}/0.0013 M pyrrole. This yielded polypyrrole samples having different chain and conjugation lengths and different concentrations of chemical defect sites. We show that both electronic and optical conductivity are affected by these changes in conjugation length and concentrations of chemical defects.

INTRODUCTION

The electronically conductive heterocyclic polymers have interesting and useful electronic, optical, and redox properties (1). For these reasons, these polymers have been the subject of considerable recent research effort. This research effort is hampered by the fact that these polymers are, in general, insoluble, intractable solids. Thus, many of the conventional methods of polymer analysis such as viscometry and gel-permeation chromatography cannot usually be applied to these materials. This is a problem because subtle changes in the conditions used to synthesize such polymers produce significant changes in the chemical characteristics of the polymer obtained (2,3). Because of the intractability of these materials, it is often difficult to explore these chemical differences.

To help address this problem, we have initiated a series of investigations aimed at systematically exploring the effects of synthetic conditions on the chemical characteristics of heterocyclic polymers. The chemical characteristics we are interested in include chain length, conjugation length, and identity and concentration of chemical defect sites on the polymer chain. We have assessed these chemical characteristics using an arsenal of analytical methodologies including X-ray photoelectron spectroscopy, fourier transform infrared spectroscopy, elemental analysis, and UV-visible spectrophotometry. Once the chemical characteristics of the polymer are known, we then correlate these characteristics with

important bulk physical properties of the polymer such as electronic conductivity and optical properties.

Thus, the general goal of this research effort is to explore the relationship between synthetic conditions and chemical characteristics of the resulting polymer and then to correlate these chemical characteristics with bulk electronic and optical properties. In this paper we show that the rate of chemical polymerization of polypyrrole can be varied by varying the concentration of monomer and initiator used to synthesize the polymer (4). We explore the effects of this variation in rate of synthesis on the chemical characteristics of the polymer. We then explore the effects of these chemical characteristics on the DC and optical conductivities of the polymer.

EXPERIMENTAL

Materials. Pyrrole (Aldrich, 99%) was distilled twice, under N_2, immediately prior to use. $FeCl_3$ (Alfa, reagent grade) and KBr (Aldrich IR, grade) were used as received. Purified water was obtained by passing house distilled water through a Millipore water purification system; this water was used as the solvent for all solutions in this study.

Polymer Synthesis. Polypyrrole (PPy) was synthesized by mixing solutions of pyrrole with solutions of $FeCl_3$ (in air) (4,5). Polymerization was allowed to proceed for 1.0 hr. Additional polymer was not obtained at longer polymerization times. The PPy formed as a black precipitate which was collected by filtration using Anopore (Alltech) microporous alumina filtration membranes.

The polymer was rinsed with water and dried for twelve hours at 23° C in vacuo. X-ray photoelectron spectroscopy showed that no $Fe^{3+/2+}$ was left in the PPy after this treatment.

Bjorklund has shown that the rate of PPy polymerization is determined by the rate of the initial electron transfer reaction

$$Py + Fe^{3+} \text{ ------> } Py^{+\cdot} + Fe^{2+} \qquad (1)$$

(4) where Py is the neutral pyrrole monomer and $Py^{+\cdot}$ is the corresponding radical cation. The rate of polymerization can, therefore, be varied by varying the initial concentrations of Py and Fe^{3+} in the polymerization solution used to synthesize the polymer. We have used this approach to prepare a series of PPy samples which were polymerized at various polymerization rates. As we will see, this gives us a series of PPy's with different chemical characteristics and electronic and optical properties.

The initial Fe^{3+} and Py concentrations used to synthesize our PPy samples are shown in Table I. Note that the initial ratio of Fe^{3+} to Py was always 50 to 1; however, the absolute concentrations were varied by over an order of magnitude. As indicated in Table I, the polymer samples are identified by the notation PPy_z, where z is the initial concentration of Fe^{3+} used in the polymerization solution. High values of z indicate that the sample was polymerized at relatively high rate.

Measurement of DC Conductivity. As indicated above, the PPy samples precipitated from the polymerization solutions as powders. These powders were pressed into pellets using an IR pellet press. A pressure of 10^4 atmospheres was used. The

conventional four-point probe method was used to obtain the DC electrical conductivities of these PPy pellets (6).

FTIR and Optical Absorption Measurements. Samples for these studies were prepared by mixing measured quantities of the various PPy powders with KBr and pressing pellets. Pellets were pressed at 10^4 atmospheres. Absorbance data were obtained on these pellets using simple transmission mode experiments. A Mattson Galaxy 4021 was used to obtain the FTIR absorption data; a resolution of 4 cm^{-1} was employed. A Perkin-Elmer Lambda spectrophotometer was used to obtain the optical absorption data. A KBr pellet devoid of PPy was used as the reference for both the FTIR and optical absorption measurements.

The FTIR data provide a wealth of information about the chemical compositions of the various PPy samples. In addition, the infra red absorption data may be used to calculate the "optical conductivity" (7) for a conductive polymer. This calculation makes use of the Drude model (7-9), which has been shown to be only qualitatively applicable to conductive polymers (10-12). For this reason, quantitative comparisons between the optical and DC conductivities are problematic. However, this method can be used to obtain information about the relative conductivities of related polymeric samples (6); an assessment of relative conductivity is all that is required here.

According to the Drude model (7), the optical conductivity (σ_{opt}) is related to the extinction coefficient for the polymer (ϵ) via

$$\sigma_{opt} = (\epsilon^2 c^2)/8\pi\omega \quad (2)$$

where ω is the frequency of the light employed. Thus, in order to calculate the optical conductivities, the extinction coefficients for our various PPy samples must be known (Equation 2). If these were homogeneous thin films of PPy, the film absorbance (A) would be related to the film extinction coefficient and the film thickness (b) via

$$A = \epsilon b \quad (3)$$

Absorption data for our PPy samples were obtained from PPy/KBr composites; thus, Equation 3 is not applicable. We can, nevertheless, calculate the extinction coefficient for the PPy within these samples by calculating an effective film thickness (β); this is the thickness of the film which would result if the PPy within the KBr pellet were compressed into a homogeneous (i.e. only PPy and no KBr) pellet. This effective film thickness is given by

$$\beta = W_{PPy}/(a\ d_{PPy}) \quad (4)$$

where W_{PPy} is the weight of PPy in the KBr pellet, a is the pellet area, and d_{PPy} is the density of the PPy.

The effective film thickness is related to the extinction coefficient of the PPy within the pellet and the experimental absorbance for the pellet via

$$A = \epsilon \beta \quad (5)$$

Thus, in analogy to the homogeneous thin film case (Equation 3) the extinction coefficient for the PPy within our KBr/PPy pellets can be obtained from the experimental absorbance data, provided β

is known. The absorbance value can then be used to calculate σ_{opt} (Equation 2).

Equation 4 shows that the density of the polymer must be known in order to calculate β. The densities for the various PPy samples were obtained by pressing pellets and measuring the dimensions and weights of these pellets. A density of 1.44 ± 0.05 g cm^{-3} was obtained for all of the PPy samples synthesized here. This is, of course, only an approximation of the density since grain boundaries between particles, if present, would add free volume to the pellet. Nevertheless, this value agrees well with a density of 1.48 g cm^{-3} reported by Hasegawa et al. (11). Finally, if the "effective film thickness" argument presented above is correct, then the absorbance for the KBr/PPy pellet should increase linearly with the weight of PPy in the pellet (combine Equations 4 and 5). Figure 1 shows that this is, indeed, the case.

X-Ray Photoelectron Spectroscopy (XPS). XPS data were obtained by mounting the PPy powders onto copper sample holders using double-sided tape. XPS spectra were acquired at 0.9 eV energy resolution on an HP 5950 ESCA spectrometer with monochromatized AlK_{α} radiation. The spectrometer was calibrated using the C1s line of graphite. Charging effects were not observed for the more highly conductive samples (i.e. samples with DC conductivities, σ_{DC}, greater than ca. 0.01 Ω^{-1} cm^{-1}). A flood gun was used for the PPy samples with $\sigma_{DC} < 0.01$ Ω^{-1} cm^{-1}.

The doping levels for the various PPy samples were

determined using XPS; the method developed by Street was employed (13). Instrumental sensitivity factors for the C1s, N1s, C12p, and O1s lines were first determined by conducting XPS analyses on a compound of known stoichiometry (Bu_4NClO_4) (13). Peak areas under the C1s, N1s, C12p, and O1s peaks for the various PPy samples were then obtained. The N and Cl data were used to obtain the doping levels. Doping levels were also determined by commercial elemental analysis (Galbraith Laboratories). The O data were used to determine the excess oxygen per pyrrole ring (see below).

Finally, prior XPS investigations of PPy have shown that high and low energy shoulders are observed on both the C1s and N1s peaks; i.e. simple gaussian-shaped peaks are never observed for PPy (13-15). Information about the chemical composition of the polymer can be obtained from the relative intensities of these high and low binding energy shoulders. Intensities for the various components of the XPS peaks were obtained by deconvolving the complex peak shape into its component gaussians. The "automatic fitting" program included with the XPS spectrometer was employed. This program provides the peak positions, peak areas, and full-widths at half maxima for the component gaussians.

RESULTS AND DISCUSSION

Effect of Initial Reactant Concentration on Apparent Yield of PPy and on Polymer Chain Length. We define the apparent yield of PPy as the grams of polymer collected (by filtration) from the

polymerization solution, divided by the theoretical maximum mass of polymer which could have been obtained. (Why these are called apparent yields will be clarified, below.) The theoretical maximum was calculated from the known quantity of monomer added to the polymerization solution, assuming that the resulting polymer has the formula $-(PyCl_x)_n-$, where x is the doping level (see Table IV).

As indicated in Table I, the apparent yield of PPy decreases with the initial reactant concentration. Because the rate of polymerization also decreases with initial reactant concentration (4), one possible explanation for the loss in yield is that the polymerization reaction had not reached completion for the low reactant-concentration solutions; however, longer reaction times did not result in the formation of additional polymer. The decrease in apparent yield is, instead, due to the formation of soluble PPy oligomers which are not collected by filtration. (This is why the term "apparent" yield is used.)

Figure 2 shows absorption spectra for filtrate solutions obtained after polymer synthesis. The solutions have been diluted so that the concentration of $FeCl_3$ in each case is 0.07 M. The spectra for a virgin 0.07 M $FeCl_3$ solution is also shown in Figure 2 (curve a), for comparison. Curve b in Figure 2 is the filtrate for sample $PPy_{1.0}$; this sample was polymerized at high rate and the apparent yield of polymer is 94% (Table I). The absorption spectrum for this filtrate is essentially identical to that of the virgin $FeCl_3$ solution, indicating that

additional chromophores (i.e. polymer) are not present in the filtrate solution. This is, of course, consistent with the high yield of polymer obtained.

The absorption spectrum for the filtrate obtained from a sample polymerized at low rate is dramatically different (curve C in Figure 2). The absorbance at all wavelengths is substantially higher and this filtrate shows the increase in absorbance with increasing wavelength characteristic of doped PPy (see e.g. (10) and Figure 5). These data show that soluble PPy is present in the solutions polymerized at low rate; this is why the (apparent) yield is lower for these samples (Table I).

The soluble polymer present in the filtrate (Figure 2 c) suggests that shorter polymer chains are obtained when PPy is synthesized at low polymerization rates; i.e at low reactant concentrations. This indicates that the rate of progagation of the nascent PPy chains becomes slower (relative to the rate of termination), when the initial concentration of reactants is decreased. Diaz has suggested that nascent PPy chains terminate via reaction with water to form a terminal carbonyl group (16); this seems particularly likely when water is used as the solvent. If termination via formation of carbonyl is correct, then the polymers synthesized at low reactant concentrations (shorter chains) should have higher concentrations of carbonyl defects. This supposition can be tested spectroscopically.

Figure 3 shows FTIR spectra for three of the PPy samples. These spectra were obtained from PPy/KBr pellets which contained

the same quantity of PPy. All three spectra show a weak band at 1705 cm^{-1}. (We will have more to say about the other bands in these spectra later.) This band has been observed in oxygen-oxidized (17), and in electrochemically over-oxidized (18) PPy, and has been attributed to carbonyl (18,19). Figure 3 shows that the intensity of this band increases as the concentration of reactants used to synthesize the polymer decreases. Thus, in agreement with the proposed termination process (16), the FTIR data indicate that carbonyl is present in our PPy samples, and that the concentration of this defect is higher in the shorter chain samples.

Figure 4 shows the C1s XPS spectra for two of the PPy samples. Both spectra show the presence of a high binding energy shoulder at 287.7 eV. This shoulder has been attributed to disorder carbons, (13) shake-up (13,14), fermi level electron excitation (20,21) and carbonyl (22,23). We will show, below, that the area under the component guassian centered at 287.7 eV scales with the intensity of the carbonyl band in the FTIR. Hence, there is no doubt that part of the XPS signal at 287.7 eV is due to carbonyl. Thus, the XPS data also support the proposed termination mechanism (16).

As indicated in Figure 4, we have conducted line shape analyses which break the total XPS signal into its various component signals. If we assume (vide infra) that the entire signal at 287.7 eV is due to carbonyl, the ratio of the area under this peak to the total C1s area, provides the quantity of

carbonyl present in the sample (23). Table II shows the results of this analysis in terms of the number of carbonyls per pyrrole ring. Because we are assuming that all of the intensity under the 287.7 band is due to carbonyl, we call these "apparent" carbonyl per ring values; as will be discussed below, these values are undoubtedly over estimates.

In agreement with our prediction (and the FTIR data), the PPy samples synthesized from low reactant-concentration solutions (shorter polymer chains) have higher concentrations of carbonyl defects than samples synthesized from the high reactant-concentration solutions (longer chains). Indeed, in comparing Tables I and II, we find that both the relative yield and the apparent number of carbonyl defects are relatively constant for samples $PPy_{2.0}$, $PPy_{1.0}$, and $PPy_{0.5}$ but change markedly for samples $PPy_{0.25}$, $PPy_{0.13}$, and $PPy_{0.06}$.

Again, it is important to emphasize that the carbonyl-per-ring values shown in Table II are only approximate because we are assuming that all of the XPS intensity at 287.7 eV is attributable to carbonyl (vide supra). Furthermore, XPS is a surface technique and it is in principle possible that the concentration of carbonyl defects is higher on the surface of the PPy sample. Hence, the values presented in Table II are undoubtedly over estimates of the concentrations of carbonyl defects in these samples. The trend toward higher concentrations of carbonyl defects for the shorter chains is, however, accurate as it is corroborated by the FTIR analysis.

It is difficult to quantify the FTIR analysis for carbonyl because the extinction coefficient for the carbonyl band is unknown. However, the integrated absorption intensity of this band can provide a relative measure of the carbonyl concentration. To be consistent with the XPS data (Table II) we assigned the area under the 1705 cm^{-1} band for $PPy_{0.06}$ an apparent carbonyl-per-ring value of 0.56. The other carbonyl-per-ring values were then calculated from this assigned value and the respective areas under the 1705 cm^{-1} bands for these PPy samples (Table II). As indicated above, this FTIR-based analysis also indicates that the carbonyl concentration increases as the reactant concentration used to synthesize the polymer decreases.

Charge Delocalization. Tian and Zerbi have recently conducted a theoretical analysis of the vibrational spectra of pristine and doped PPy; their calculations are based on a concept they call the effective conjugation coordinate (24,25). This theory successfully predicts the number and positions of the main IR bands in PPy and also predicts how the intensities and positions of these bands change with the extent of delocalization in the polymer chain (25). The bands at 1560 and 1480 cm^{-1} (Figure 3) are especially affected by changes in the extent of delocalization. These changes can be most easily visualized by ratioing the integrated absorption intensity of the 1560 cm^{-1} band to the integrated absorption intensity of the 1480 cm^{-1} band. We call this ratio I_{1560}/I_{1480}.

According to Tian and Zerbi's analysis, I_{1560}/I_{1480} is

inversely proportional to the extent of delocalization (25). Table III shows experimental I_{1560}/I_{1480} ratios for the polymers synthesized here. I_{1560}/I_{1480} increases as the concentration of reactants used to synthesize the polymers decreases. This suggests that the extent of delocalization increases with concentration of reactants used to synthesize the PPy.

Optical absorption data can also be used to obtain a relative assessment of the extent of delocalization. Figure 5 shows absorption spectra for our PPy samples. In agreement with previously observed results (26,27), these spectra show two broad bands, one centered approximately at 450 nm and one centered roughly at 900 nm. According to Street et al. the simplified band diagram shown in Figure 6 applies to doped PPy (26,27). The 450 nm and 900 nm peaks correspond to the transitions labeled VB-->ABB and VB-->BB, respectively, in Figure 6.

The most obvious trend in the optical absorption data is the dramatic increase in absorbance for the polymers synthesized at high reactant concentrations (Figure 5). As will be discussed in detail below, this indicates that the polymers synthesized at high reactant concentrations have higher electronic conductivities (7). The absorption spectra in Figure 5 show a second important trend. The peak positions for both the VB-->ABB and the VB-->BB bands redshift as the concentration of reactant used to synthesize the sample increases.

Figure 6 shows that the sum of the vectors labeled VB-->BB and VB-->ABB is approximately equal to the band gap (26).

Therefore, the redshifts in the VB-->BB and VB-->ABB observed in Figure 5 indicates that the band gaps for these PPy samples decrease with increasing reactant concentration. Since a decrease in band gap means that the conjugation length is longer (26), these data corroborate the conclusion obtained from the FTIR data - the polymers synthesized at high reactant concentration (longer chain length polymers) have longer conjugation lengths.

Doping Level. Doping levels were determined via both XPS (see Experimental) and commercial elemental analyses. Results of both types of analyses are shown in Table IV. The agreement between the XPS and the elemental analyses is quite good. Doping level decreases monotonically from ca. 0.21 (for the sample polymerized at the highest reactant concentration), to ca. 0.07 (for the sample polymerized at the lowest reactant concentration). Thus, doping level in these polymers appears to scale with chain length. We propose the following explanation for this correlation.

The oxidation potential for pyrrole monomer is higher than that for pyrrole dimer, trimer, tetramer, and polypyrrole (26-29). Thus, the oligomeric and polymeric chains produced by oxidative coupling of pyrrole are oxidized by the excess Fe^{3+} in the polymerization solution. However, because the oxidation potentials of very short chains are higher than for longer chains, doped short chains should be more highly chemically reactive than doped long chains.

For example, doped short chains should be more susceptable to nucleophilic attack by water (16). Such reactions will undope these short PPy chains. Thus, we propose that while the shorter chain-length samples are synthesized in the doped form, their higher chemical reactivity causes them to become undoped via parasitic chemical reactions. As a result, the short chains end up with lower doping levels (Table IV).

Table IV also presents results of an alternative XPS procedure for determining the doping level in PPy. Figure 7 shows N1s XPS spectra for two of our PPy samples. A high binding energy shoulder (centered at ca. 401.3 eV) appears in these spectra. Street observed an analogous shoulder in poly(β,β'-dimethylpyrrole) and concluded that this feature arises from nitrogen atoms which bear higher positive charge than the nitrogen atoms comprising the main peak (13). Eaves et al. suggest that these "more positive" nitrogen are contained in monomer units immediately adjacent to the doping anion (30). If this is true, the fraction of nitrogen atoms bearing this excess positive charge should be equivalent to the doping level.

To test this hypothesis, we ratioed the area under the gaussian centered at 401.3 eV to the total area under the N1s peak (Figure 7). This gives the fraction of N atoms which bare excess positive charge (N^+/N). This ratio is shown, along with the doping levels, in Table IV. The N^+/N ratio is essentially identical to the doping level for all of the polymers investigated here. These data corroborate the supposition that

the positively-charged N's are contained in rings which are adjacent to the doping anions (30). Furthermore, this method for determining the doping level is more convenient than the conventional XPS method (see Experimental) because calibration of the spectrometer with a material of known stoichiometry (e.g. Bu_4NClO_4) is not necessary.

DC and Optical Conductivities. DC conductivities (σ_{DC}) for our various PPy samples are shown in Table V. Conductivity decreases monotonically from 14 S cm^{-1} (for the sample polymerized at highest reactant concentration), to $2.7x10^{-5}$ S cm^{-1} (for the sample polymerized at the lowest reactant concentration). These data are in perfect accord with the conclusions reached above concerning conjugation length and doping level - polymers synthesized at high reactant concentrations have longer conjugation lengths and higher doping levels and are thus significantly more conductive.

While both conjugation length and doping level affect conductivity (31), it is obvious that the factor of 3 change in the doping level (Table IV) cannot be the major contributor to the factor of $4x10^5$ drop in conductivity (Table V). Indeed, it is well known that in this 7 to 20 % doping level range, conductivity for PPy is relatively insensitive to doping level (32,33). Thus, the decrease in conjugation length must be the primary factor responsible for the dramatic decline in DC conductivity observed in Table V. We propose that this diminution in conductivity occurs because interchain hopping

events (29,34) contribute more strongly to the measured DC conductivity in polymers with shorter conjugation lengths.

Optical conductivity (σ_{opt}) data can be used to test this hypothesis. It is generally believed that σ_{opt} reflects the rate of the intrachain transport process rather than the rate of the (slower) interchain hopping process (29). If the diminution in σ_{DC} is due primarily to the slower interchain contribution in the polymers with shorter conjugation length, the optical conductivities will not see this effect. The σ_{opt} values should, therefore, not show the dramatic decline observed in the DC data.

Optical conductivities were obtained from the absorption spectra shown in Figure 5. Note qualitatively, first, that the higher absorbencies in the "free-carrier" range (above ca. 600 nm), for the polymers synthesized at high reactant concentrations, indicate that these polymers are more conductive. This observation agrees qualitatively with the trend observed in the σ_{DC} data (Table V). Optical conductivities obtained at 888 nm are shown in Table V. While σ_{opt} decreases for the polymers synthesized at low reactant concentration, this decrease is not nearly as dramatic as the decrease in σ_{DC}. These data corroborate the assertion that the σ_{opt} is more strongly influenced by the intrachain transport process (29) and that the extreme drop in σ_{DC} is primarily a conjugation length effect.

It is important to emphasize, however, that σ_{opt} does decrease monotonically with concentration of reactant used to synthesize the polymers (Table V). The decrease in charge

carrier density (i.e. doping level, Table IV) undoubtedly contributes to this diminution in σ_{opt}. However, the doping level changes by only a factor of three (Table IV) while the optical conductivity changes by a factor of ca. 100 (Table IV). This suggests that the conjugation lengths for the polymers synthesized at the lowest reactant concentrations are so short that the charge carriers are not free to move with the oscillating electric field of the impinging radiation. Because of this constraint, the optical conductivities for these very short conjugation length samples do not truly reflect the facility of the intrachain transport process.

We have already noted that the I_{1560}/I_{1480} ratio (Table III) is related to the extent of delocalization. Furthermore, conductivity is also critically dependent on delocaliztion. Hence, there should be a relationship between I_{1560}/I_{1480} and conductivity. Figure 8 shows a plot of $\log(\sigma_{DC})$ vs. I_{1560}/I_{1480}. The data were obtained from the polymers described here and from a "template-synthesized" (35,36) 30 nm-diameter PPy fibril. Figure 8 shows that $\log(\sigma_{DC})$ is linearly related to I_{1560}/I_{1480} over a σ_{DC} range of <u>seven orders of magnitude</u>. Figure 8 is important because these data indicate that the DC conductivity of a PPy sample can be obtained from a simple FTIR measurement.

<u>Other Chemical Defects</u>. We have obtained spectroscopic evidence for the presence of three other chemical defects. Again, the concentrations of these defects are dependent on the concentration of reactant used to synthesize the PPy. Table VI

shows concentrations for two of these defects, in terms of number of defect sites per pyrrole ring.

The first entry in Table VI is excess oxygen per ring. Excess oxygen is defined as oxygen in excess of the oxygen tied up as carbonyl (Table II). Table VI shows that there is ca. one excess O per every three rings for the polymers synthesized at high reactant concentration, and greater than one excess O for every two rings in the polymers synthesized at low reactant concentration. This is a lot of excess oxygen. Similarly high amounts of excess oxygen have been observed for electrochemically-synthesized PPy (37). To date, there has been no satisfactory explanation for this excess oxygen.

We have recently conducted FTIR analyses on reduced (i.e. nonconductive) electrochemically-synthesized PPy films (38). Spectra for the reduced material show prominent bands at 1119 cm^{-1} (C-O stretch) and 3558 cm^{-1} (O-H stretch), indicating that these polymers contain large quantities of -OH (38). In the oxidized (conductive) material, these bands are completely obscured by the free-carrier absorption. These bands are observed in PPy electrochemically synthesized in acetonitrile containing 2 % water. However, they are not observed in PPy synthesized in rigorously-dried acetonitrile. These investigations suggest that the excess O in the PPy samples described here (and in all PPy samples synthesized in water or solvents containing trace water) is from -OH.

The second defect reported in Table VI is -C=N- (39). The

N1s XPS spectra show a clearly resolved shoulder at 397.5 eV (Figure 7); this shoulder has been attributed to -C=N- (14). The ratio of the area under the gaussian center at 397.5 to the total N1s area, provides the number of -C=N- defects per pyrrole ring (Table VI). The polymers synthesized at low reactant concentrations contain higher concentrations of -C=N- defects. This is important because these defects interrupt conjugation and thus contribute to the shorter conjugation lengths in the PPy synthesized at low reactant concentrations.

The final chemical defect-type which clearly appears in the polymers synthesized at low reactant concentrations is the sp^3 defect. Figure 9 shows FTIR spectra in the region form 4,000 to 2,000 cm^{-1} for four of our PPy samples. Note that the samples synthesized at low reactant concentration show weak bands at 2,931 and 2850 cm^{-1}, characteristic of the C-H stretch for sp^3 carbon. Because sp^3 defects are associated with the carbonyl chain termini (17), it is not surprising that these short chain polymers should show high concentrations of these defects.

The 2931 and 2850 cm^{-1} peaks are not observed for the polymers synthesized at high reactant concentrations (Figure 9). While it would be logical to assume that this is because there are fewer of these defects in these longer chain-length polymers, it is possible that these vibrations are masked by the strong free-carrier absorption for these more highly-conductive materials (Figure 9).

CONCLUSIONS

We have shown that through control of the polymerization conditions, polypyrrole with different chemical characteristics can be obtained. We have correlated these chemical characteristics with the electronic and optical properties of the various polymers. We will expand on this general theme of correlations between synthetic conditions, chemical characteristics, and electronic and optical properties in future publications.

ACKNOWLEDGEMENTS

This work was supported by the Office of Naval Research and the Air Force Office of Scientific Research. We would like to acknowledge valuable discussions with Dr. Wenbin Liang.

References:

1. T. A. Skotheim, Ed. "Handbook of Conducting Polymers", Dekker, NY, 1986, Vol. I, Chaps. 3, 8, 9, 10, 15, 19.
2. R. M. Penner and C. R. Martin, J. Phys. Chem., 93, 984 (1989).
3. C. R. Martin and L. S. VanDyke in Molecular Design of Electrode Surfaces, R. W. Murry Ed., Wiley, NY, in press.
4. R. B. Bjorklund, J. Chem. Soc., Faraday Trans. 1, 83, 1507 (1987).
5. A. Pron, Z. Kucharski, C. Budrowski, M. Zagorska, S. Krichene, J. Suwalski, G. Dehe, and S. Lefrant. J. Chem. Phys., 83, 5923 (1985).
6. G. Tourillon and F. Garnier, J. Phys. Chem., 87, 2289 (1983).
7. J. C. W. Chien, Polyacetylene, Academic Press, NY, pp. 551-552, 1984.
8. J. Simon and J. J. Andre, Molecular Semiconductors, Springer-Verlag, NY, pp. 8-17, 1985.
9. F. Abeles, Optical Properties of Solids, North-Holland, Amsterdam, pp. 143-145, 1972.
10. K. Yakushi, L. J. Lauchlan, T. C. Clark, G. B. Street, J. Chem. Phys., 79, 4774 (1983).
11. S. Hasegawa, K. Kamiya, J. Tanaka, M. Tanaka, Synth. Met., 14, 97 (1986).
12. C. R., Jr. Fincher, M. Ozaki, M. Tanaka, D. Peebles, L. J. Lauchlan, A. J. Heeger, A. G. MacDiarmid, Phys. Rev. B, 20, 1589 (1979).
13. P. Pfluger and G. B. Street, J. Chem. Phys, 80, 544 (1984).
14. T. A. Skotheim, M. I. Florit, A. Melo, and E. O'Grady, Phys. Rev. B, 30, 4846 (1984).
15. G. Tourillon and Y. Jugnet, J. Chem. Phys., 89, 1905 (1988).
16. A. F. Diaz and J. Barcon, in "Handbook of Conducting Polymers", T. A. Skotheim, Ed., pp 81, Marcel Dekker, Inc., NY, 1986.

17. G. B. Street, T. C. Clarke, M. Krounbi, K. Kanazawa, V. Lee, P. Pfluger, J. C. Scott, and Weiser, Mol. Cryst. and Liq. Cryst. 83, 253 (1982).
18. F. Beck, P. Braun, and M. Oberst, Ber. Bunsenges. Phys. Chem., 91, 967 (1987).
19. G. Gustafsson, I. Lundstrom, B. Liedberg, C. R. Wu, O. Inganas, and O. Wennerstrom, Synth. Met., 31, 163 (1989).
20. W. R. Salaneck, R. Erlandsson, J. Prejza, I. Lundstrom, and O. Inganas, Synth. Met., 5, 125 (1983).
21. S. Hino, K. Iwasaki, H. Tatematsu, and K. Matsumoto, Bull. Chem. Soc. Jpn., 63, 2199 (1990).
22. R. Erlandsson, O. Inganas, Lundstrom and W.R. Salaneck, Synth. Met. 10 303 (1985).
23. H. Munstedt, Polymer, 29, 296 (1988).
24. G. Zerbi, C. Castiglioni, J. T. Lopez Navarrete, B. Tian, M. Gussoni, and G. Zerbi, Synth. Met. 28, D359 (1989).
25. B. Tian, and G. Zerbi, J. Chem. Phys. 9[illegible], [illegible]92 (1990).
26. J. L. Bredas and G. B. Street, Acc. Chem. Res., 18, 309 (1985).
27. J. L. Bredas, J. C. Scott, K. Yakushi, and G. B. Street, Phys. Rev., 30, 1023 (1984).
28. A. F. Diaz, J. Crowley, J. Bargon, G. P. Gardini, and J. B. Torrance, J. Electroanal. Chem., 121, 355 (1981).
29. K. Tanaka, T. Shichiri, M. Toriumi, and T. Yamabe, Synth. Met. 14, 271 (1986).
30. J. G. Eaves, H. S. Munro, and D. Parker, Polym. Commun. 28, 38 (1987).
31. H. Shirakawa and H. Nemoto, Polym. Prep. Jpn, 31, 372 (1982).
32. D. Moses, A. Denenstein, J. Chen, A. J. Heeger, P. MacAndrew, T. Woerner, A. G. MacDairmid, and Y. W. Park, Phys. Rev. B, 25, 7652 (1982).
33. B. J. Feldman, P. Burgmayer, and R. W. Murray, J. Am. Chem. Soc., 107, 872 (1985).
34. S. Roth, H. Bleier, and W. Pukacki, Faraday Discuss. Chem. Soc., 88, 223 (1989).

35. Z. Cai and C. R. Martin, J. Am. Chem. Soc., 111, 4138 (1989).

36. C. R. Martin, L. S. VanDyke, Z. Cai, J. Am. Chem. Soc., 112, 8976 (1990).

37. P. Pfluger, M. Krounbi, and G. B. Street, J. Chem. Phys., 78, 3212 (1983).

38. J. T. Lei, W. Liang, and C. R. Martin, manuscript in preparation.

39. O. Inganas, R. Erlandsson, C. Nylander, and I. Lundstrom, J. Phys. Chem. Solids, 45, 427 (1984).

Table I. Concentrations used to synthesize the various polypyrrole samples and apparent[a] yields obtained.

Sample Designation	$[Fe^{3+}]$ (M)	[Pyrrole] (M)	Apparent[a] Yield
PPy_2	2.0	0.040	0.95
PPy_1	1.0	0.020	0.94
$PPy_{0.5}$	0.5	0.010	0.87
$PPy_{0.25}$	0.25	0.0050	0.71
$PPy_{0.13}$	0.13	0.0025	0.51
$PPy_{0.06}$	0.06	0.0013	0.40

[a] See text

Table II. Apparent[a] number of carbonyl defects per ring as estimated by XPS and FTIR.

	Polymer					
Method	PPy_2	PPy_1	$PPy_{0.5}$	$PPy_{0.25}$	$PPy_{0.13}$	$PPy_{0.06}$
XPS	0.23	0.20	0.20	0.28	0.33	0.56
FTIR/ XPS	0.18	0.15	0.15	0.30	0.41	0.56

[a] See text.

Table III. Ratio of the integrated absorption intensities of the 1560 cm^{-1} and 1480 cm^{-1} FTIR bands (I_{1560}/I_{1480}).

Polymer	---	$PPy_{2.0}$	$PPy_{1.0}$	$PPy_{0.25}$	$PPy_{0.13}$	$PPy_{0.06}$
I_{1560}/I_{1480}	---	3.8	4.5	5.4	7.1	8.5

Table IV. Doping levels measured by XPS and elemental analysis and N^+/N ratios[a] as determined by XPS.

	Polymer					
	PPy_2	PPy_1	$PPy_{0.5}$	$PPy_{0.25}$	$PPy_{0.13}$	$PPy_{0.06}$
Doping Level (XPS)	0.21	0.19	0.18	0.13	0.10	0.07
Doping Level (Elemental analysis)	0.24	0.21	0.21	0.15	0.11	0.10
N^+/N Ratio[a]	0.26	0.21	0.18	0.11	0.09	0.08

[a] See text.

Table V. DC and optical conductivities (σ_{DC} and σ_{opt}).

	Polymer					
	PPy_2	PPy_1	$PPy_{0.5}$	$PPy_{0.25}$	$PPy_{0.13}$	PPy0.06
σ_{DC} (Ω^{-1} cm^{-1})	14.1	6.2	0.81	7.4×10^{-3}	1.1×10^{-4}	2.7×10^{-5}
$\sigma_{opt.}$ (Ω^{-1} cm^{-1})	26.7	13.4	1.7	0.85	0.53	0.18

Table VI. Excess oxygen[a] and -C=N- per pyrrole ring.

	Polymer					
	PPy_2	PPy_1	$PPy_{0.5}$	$PPy_{0.25}$	$PPy_{0.13}$	PPy0.06
Excess O[a] per ring	0.27	0.28	0.30	0.32	0.65	0.54
-C=N- per ring	0.06	0.06	0.11	0.12	0.16	0.18

[a] See text.

Figure Captions

1. Absorbance of PPy/KBr pellets vs. amount of PPy (in mg) incorporated into the pellet. a. Absorbance at 4000 cm^{-1}. b. Absorbance at 1564 cm^{-1}.
2. Absorption spectra for a. 0.07 M $FeCl_3$. b. Filtrate solution from sample PPy_1. c. Filtrate solution form sample $PPy_{0.06}$. The filtrates were diluted such that the Fe^{3+} concentration in each case was 0.07 M.
3. Infrared spectra in the 2000 to 600 cm^{-1} window for three PPy samples. The equivalent thickness (see text) for all three samples was 0.6 μm. The samples were a. = PPy_2, b. = PPy_1, c. = $PPy_{0.06}$.
4. Representative C1s core level XPS spectra. a. PPy_1. b. $PPy_{0.06}$.
5. Absorption spectra for various PPy samples. Samples and equivalent thicknesses (see text) were a. PPy_2 (0.32 μm), b. PPy_1 (0.48 μm), c. $PPy_{0.5}$ (0.48 μm), d. $PPy_{0.25}$ (0.55 μm), e. $PPy_{0.13}$ (0.34 μm).
6. Simplified band structure diagram for doped polypyrrole.
7. Representative N1s core level XPS spectra. a. PPy_1. b. $PPy_{0.06}$.
8. Log of the DC conductivity vs. I_{1560}/I_{1480} (see text) for the six PPy samples investigated here and for a 30 nm-diameter template-synthesized PPy fibril (highest point, see reference (34)).
9. Infrared spectra in the 4000-2000 cm^{-1} window for three PPy samples. The equivalent thickness (see text) for all three samples was 0.6 μm. The samples were a. = PPy_1, b. = $PPy_{0.25}$, c. = $PPy_{0.13}$, d = $PPy_{0.06}$.

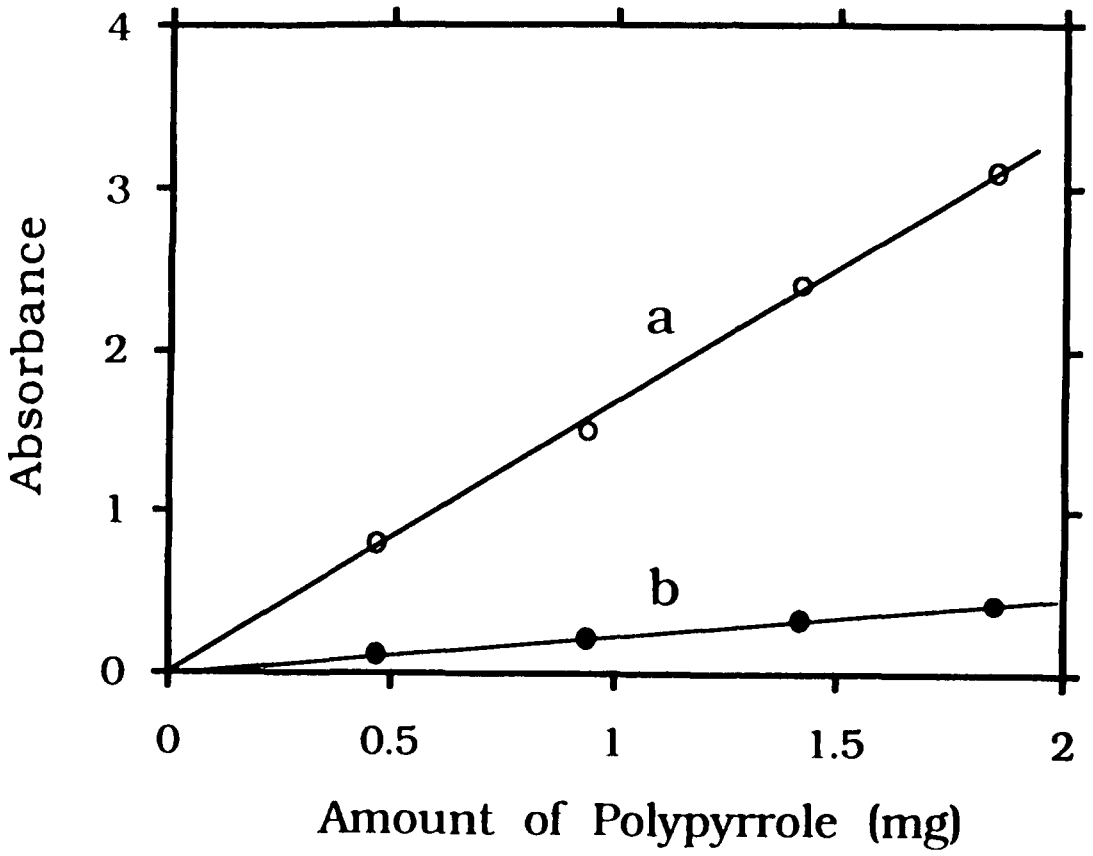

Fig 1

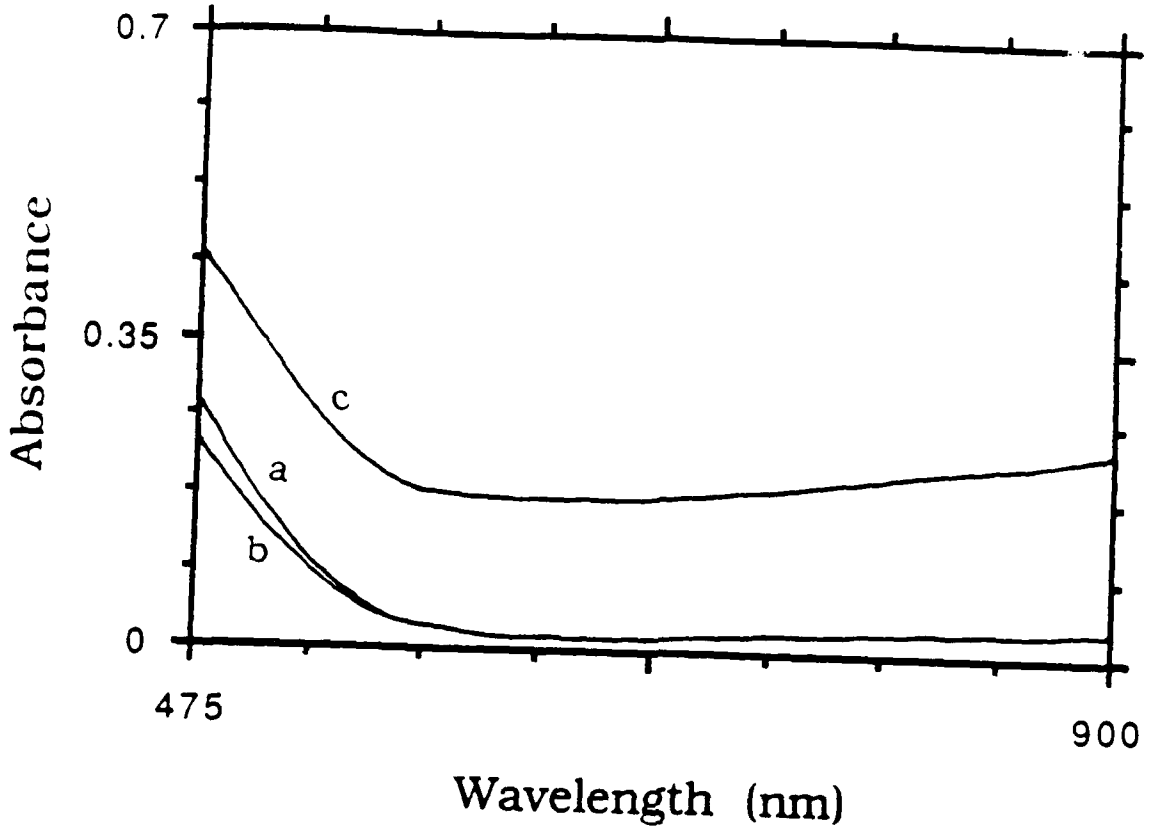
0.7
0.35
0
Absorbance
c
a
b
475
900
Wavelength (nm)

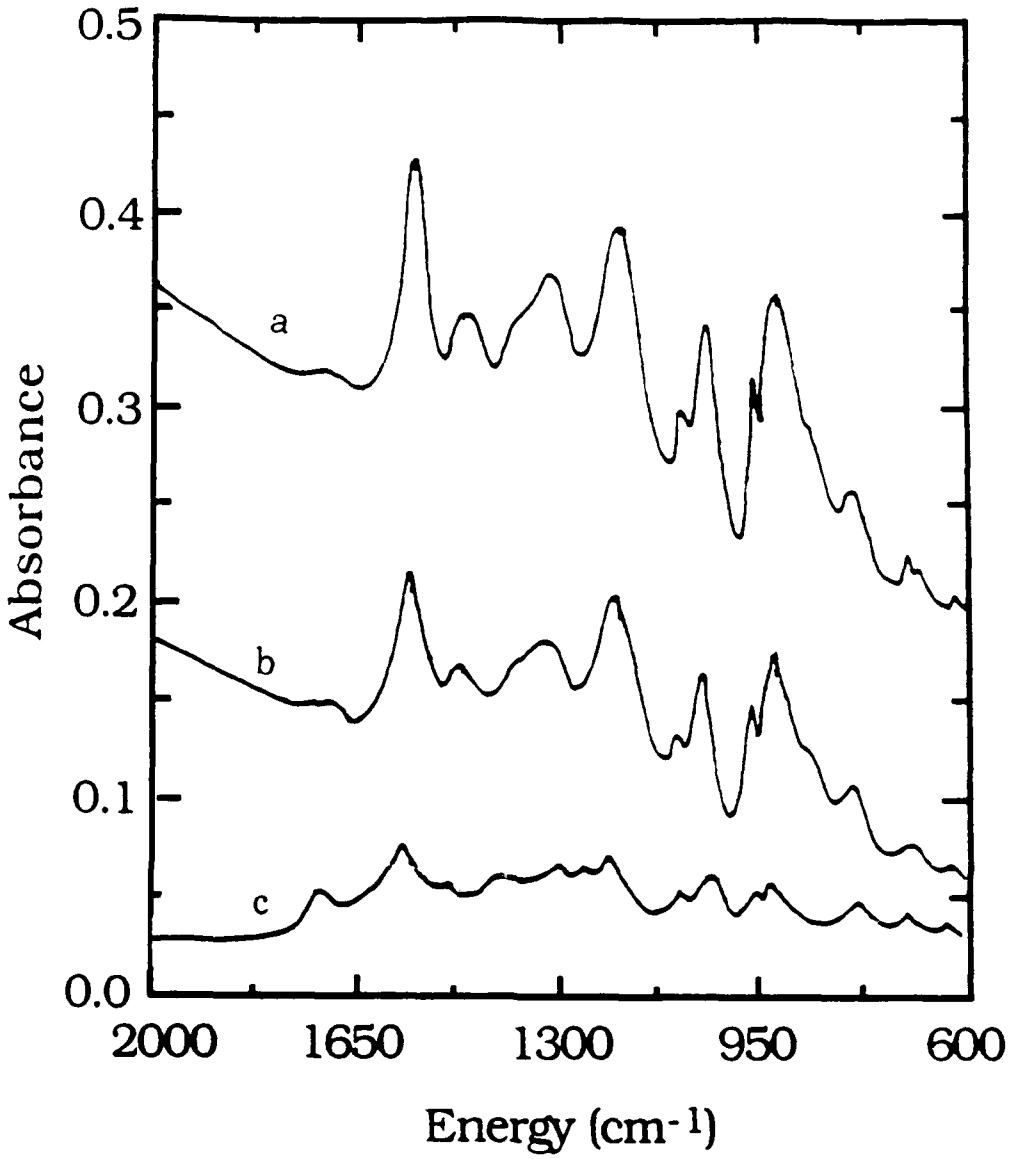
0.5
0.4
0.3
0.2
0.1
0.0
Absorbance
a
b
c
2000
1650
1300
950
600
Energy (cm-1)

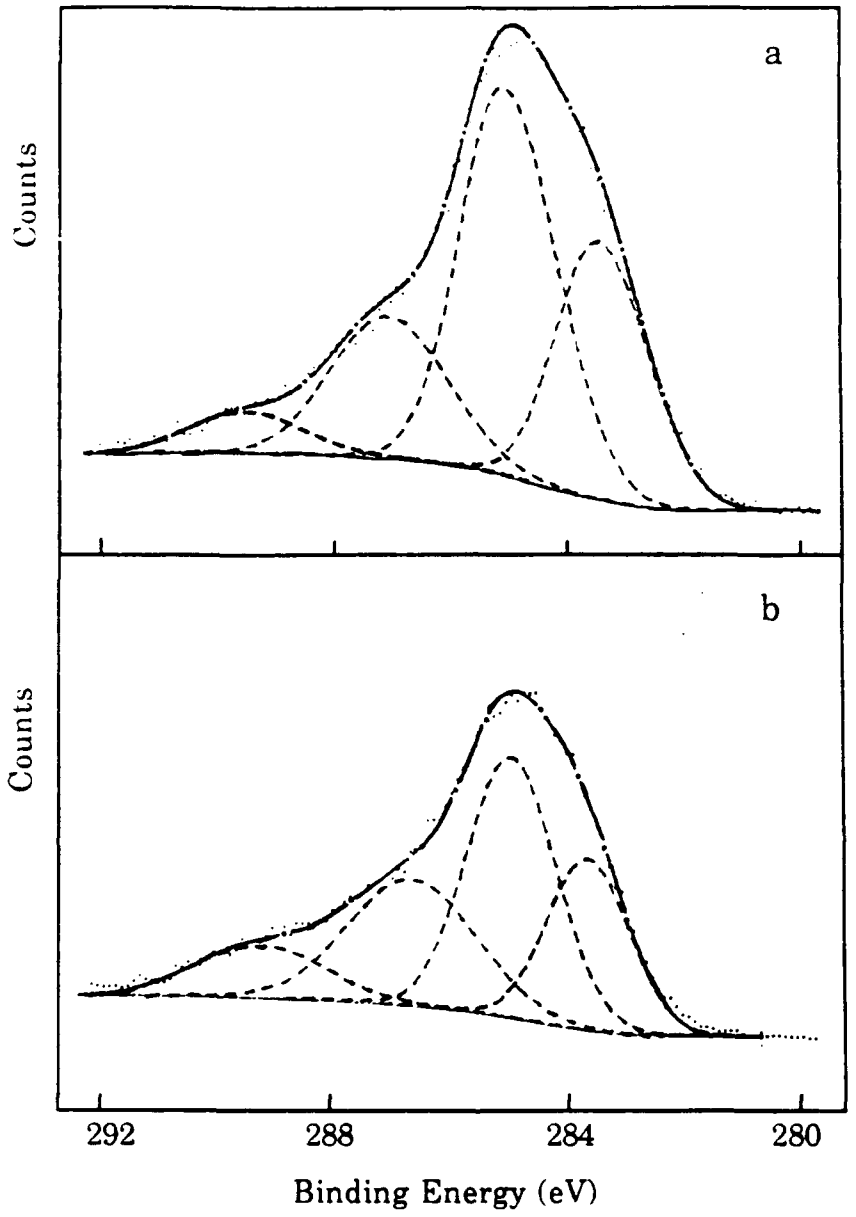

Fig 4

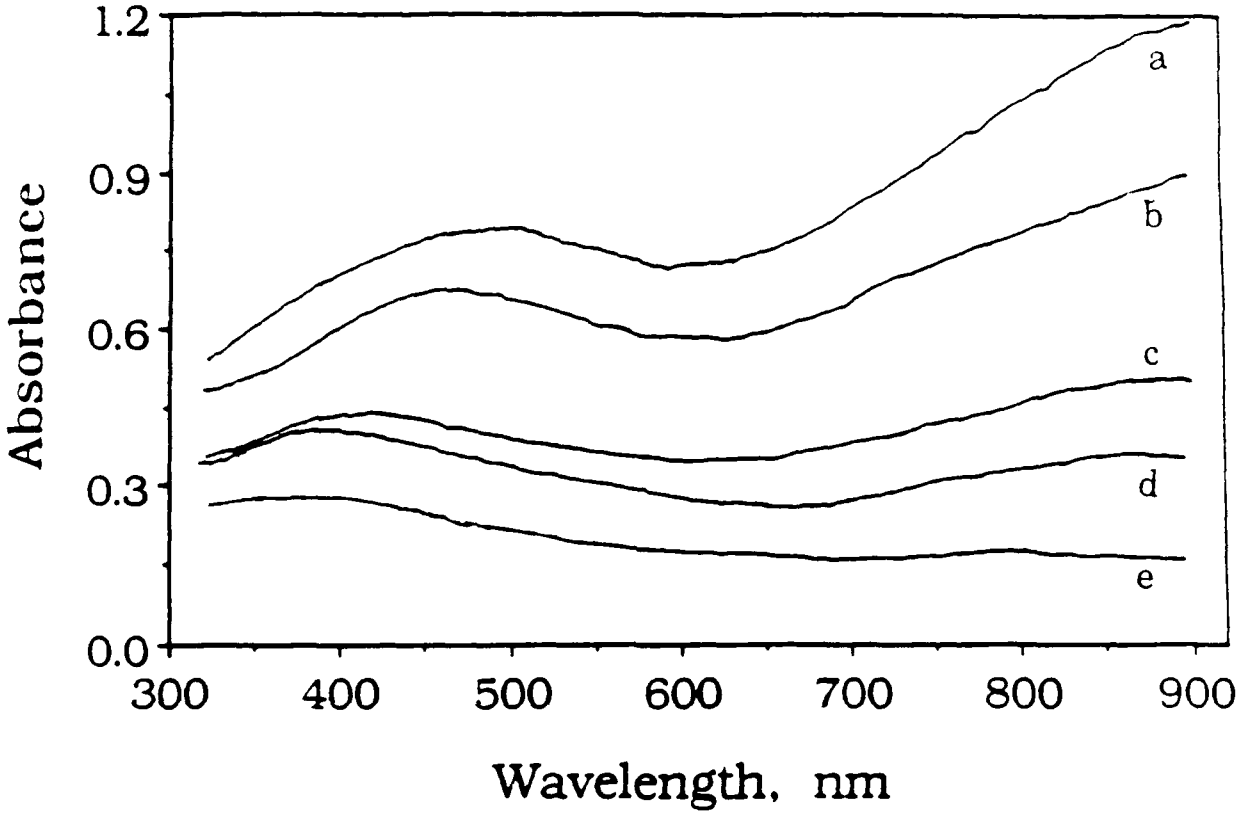
1.2
0.9
0.6
0.3
0.0
Absorbance
300
400
500
600
700
800
900
Wavelength, nm
a
b
c
d
e

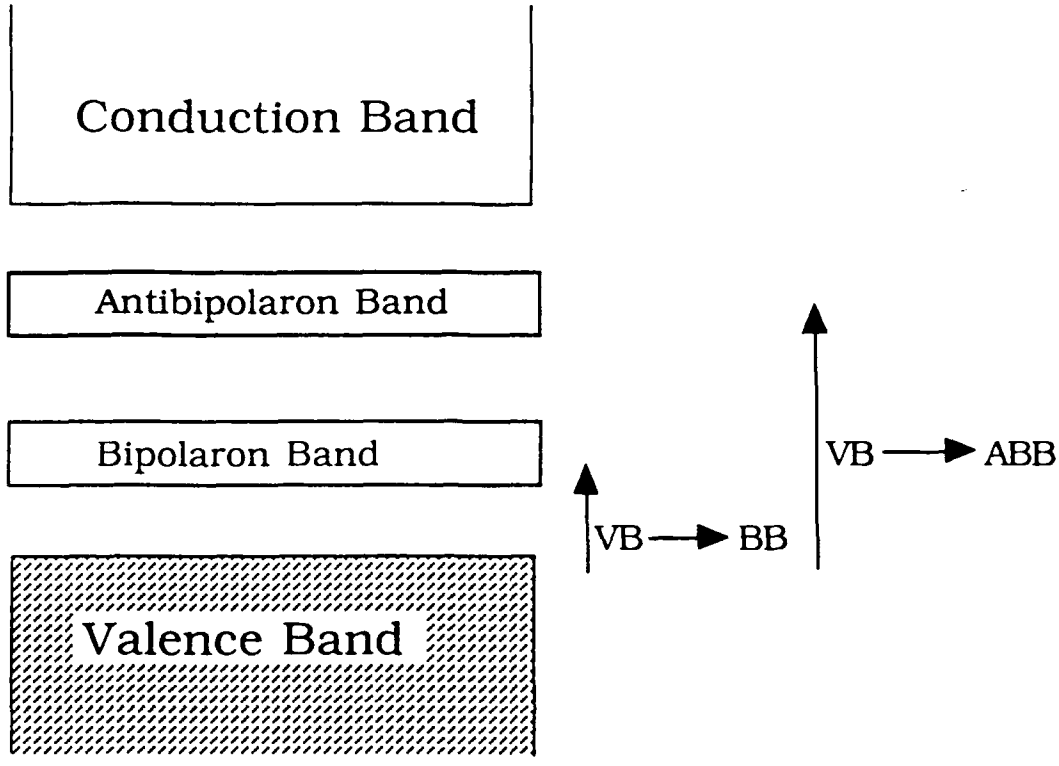
Conduction Band
Antibipolaron Band
Bipolaron Band
Valence Band
VB → BB
VB → ABB

Fig. 5

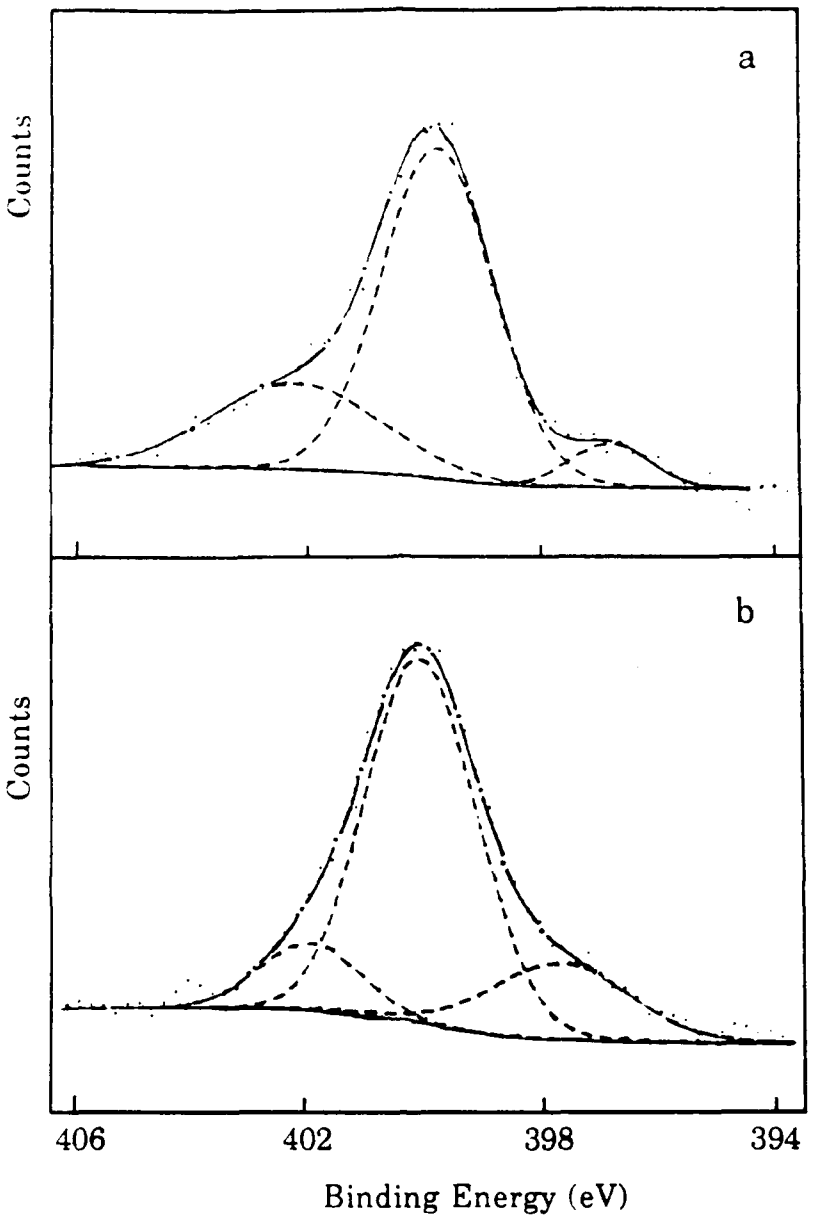

Fig 7

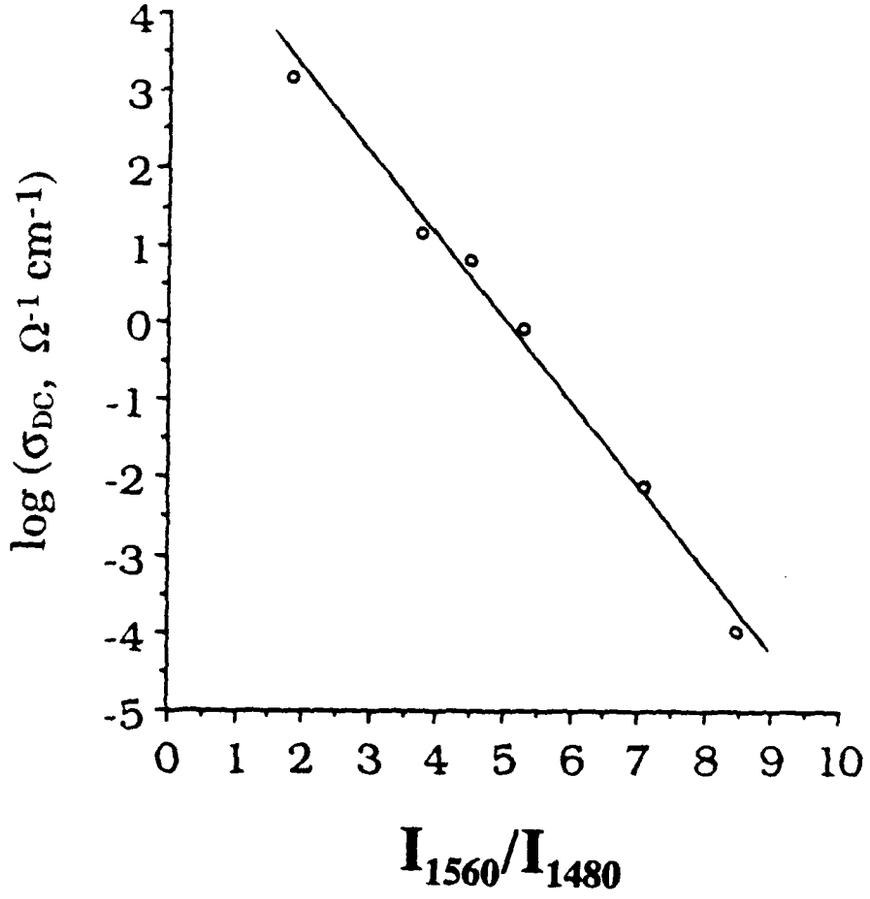
log (σ_{DC}, Ω^{-1} cm^{-1})
4
3
2
1
0
-1
-2
-3
-4
-5
0 1 2 3 4 5 6 7 8 9 10
I_{1560}/I_{1480}

Fig:

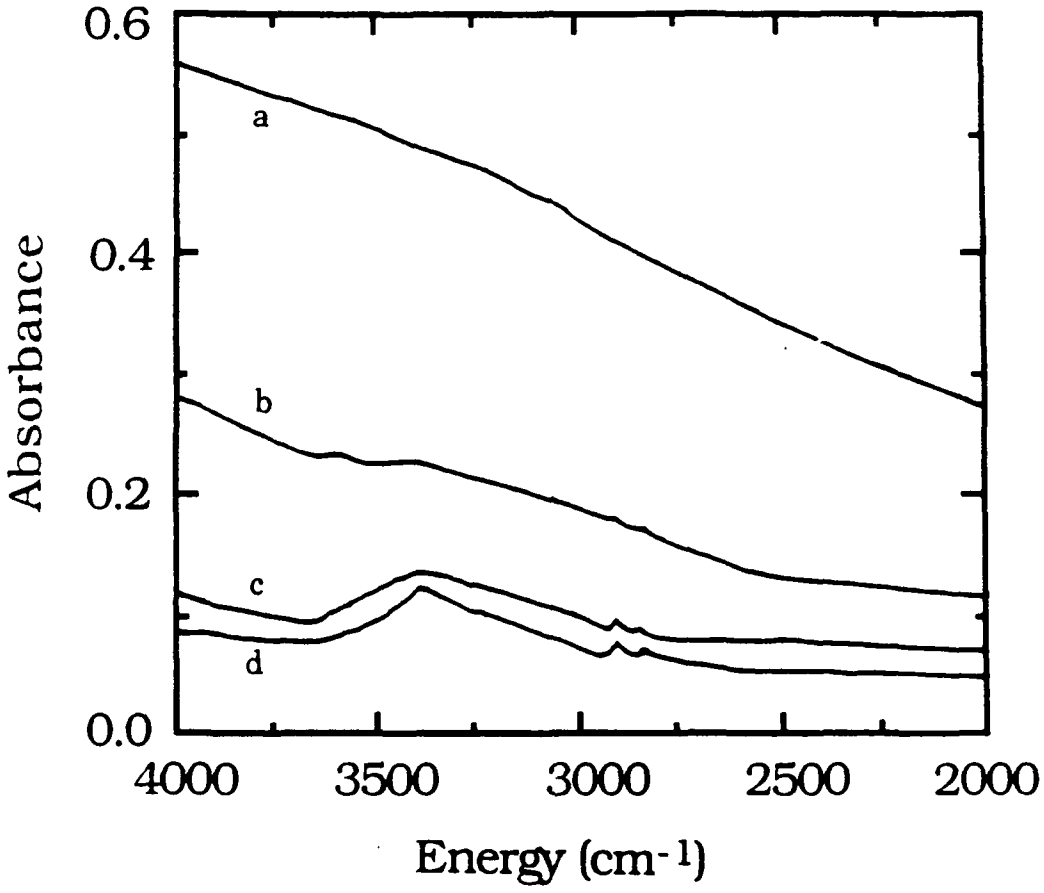
0.6
0.4
0.2
0.0
Absorbance
a
b
c
d
4000
3500
3000
2500
2000
Energy (cm-1)